# Relating brain functional connectivity to anatomical connections: Model Selection

Fani Deligianni[1], Gael Varoquaux[2,3], Bertrand Thirion[3], Emma Robinson[1], David J. Sharp[4], A. David Edwards[5], Daniel Rueckert[1]

[1] Department of Computing, Imperial College London, UK
[2] INSERM U922, Neurospin, CEA Saclay, France
[3] Parietal project team, INRIA, Saclay, France
[4] C3NL, Division of Experimental Medicine, Imperial College London, UK
[5] Institute of Clinical Sciences, Imperial College London, UK

**Abstract.** We aim to learn across several subjects a mapping from brain anatomical connectivity to functional connectivity. Following [1], we formulate this problem as estimating a multivariate autoregressive (MAR) model with sparse linear regression. We introduce a model selection framework based on cross-validation. We select the appropriate sparsity of the connectivity matrices and demonstrate that choosing an ordering for the MAR that lends to sparser models is more appropriate than a random. Finally, we suggest randomized Least Absolute Shrinkage and Selective Operator (LASSO) in order to identify relevant anatomo-functional links with better recovery of ground truth.

## 1 Introduction

Disruption of brain connectivity have been implicated in a number of diseases [2] including schizophrenia [3], autism [4] and brain trauma [5]. This has spurred interest in network organization and dynamics, studied with diffusion weighted MRI (DWI) or resting-state functional MRI (rs-fMRI) [6]. Multi-modal imaging, integrating both functional and anatomical descriptions can yield a more detailed picture of brain architecture and dramatically improve our understanding of brain function and malfunction [7]. Model-based studies have shown links between anatomical and functional whole-brain connectivity [8, 9]. However, there has been limited work on a systematic framework to investigate whole-brain interactions between structure and function. Most of current studies limit their analysis within specific networks and thus they are based on a-priori hypotheses, which ignore influences from other areas [10, 11]. Here we investigate data-driven predictive modeling from anatomical to functional networks to uncover mechanisms ignored in studies with a-priori defined interactions.

We set the problem as the prediction of whole-brain resting-state functional connectivity from anatomical brain connectivity. In a population of $S$ subjects, we consider the connectivity between a set of $N$ regions of interest (ROIs). Our supervised learning task is to link across subjects the anatomical connections

between these brain regions, as estimated by tractography, to functional connections, *i.e.* the observed synchronization in the brain activity observed via rs-fMRI. We represent the set of anatomical connections for a subject $s$ as a symmetric connectivity matrix $\boldsymbol{A}^s \in \mathcal{S}ym_N$. The corresponding brain activity in the ROIs is summarized by $N$ time series of length $t$, $\boldsymbol{X}^s \in \mathbb{R}^{N \times t}$. We want to explain the correlation structure of the observed fMRI time-series $\boldsymbol{X}^s$ from the subject's anatomical connectivity matrix $\boldsymbol{A}^s$.

In [1] we introduced a learning framework using multiple penalized regression to link $\boldsymbol{A}^s$ and the covariance matrix of the fMRI data $\boldsymbol{\Sigma}^s \in \mathbb{R}^{N \times N}$. The generative model of the functional signal relies on autoregressive Gaussian processes spanning a graphical model, the Markov structure of which is restricted by the anatomical connectivity. Estimating the fMRI model is then a covariance selection problem, computing the maximum likelihood estimate of the precision –inverse covariance– matrix, $\boldsymbol{K}$ parameterize a multivariate Gaussian model, subject to the conditional independence constraints. The output space of the regression from anatomical to functional connectivity, is then the set of symmetric positive definite (SPD) matrices. We take an unconstrained parametrization of SPD matrices using a matrix square-root of the precision matrix $\boldsymbol{K}$ to be predicted. To do that we use a Cholesky decomposition of $\boldsymbol{K}$, which is not invariant by a permutation of the rows and columns of $\boldsymbol{K}$.

Firstly, we address the selection of the optimal ordering in this framework. Using cross-validation we show that a permutation of $\boldsymbol{K}$ that favors a sparser Cholesky decomposition results in higher prediction performance than a random ordering. Subsequently, we select the optimal sparsity of the joint anatomical and functional graphs. Finally, we introduce the randomized Least Absolute Shrinkage and Selective Operator (Lasso) for model identification. This results in the recovery of the underlying anatomo-functional links with a conservative control of false positives in a multiple testing framework. Moreover, it is less sensitive to the regularization parameters and it assigns a probability to each connection, with an intuitive and straightforward interpretation.

## 2 Generative model and learning strategy

In this section, a Gaussian graphical model describes the generative rs-fMRI process and the Markov network independencies are introduced based on the structural connectivity. The prediction framework is based on sparse penalised linear regression and an intuitive way to derive SPD matrices based on Cholesky decomposition of the precision matrix.

### 2.1 Generative model.

We use graphical models of autoregressive Gaussian models to describe the generative process of fMRI time series. A graphical model of the fMRI time series is an undirected graph with nodes equal to the number of ROIs. Each pair of nodes is connected with an edge if the underline time series are conditionally

dependent, given the other time series. This is equivalent to multivariate autoregressive models (MAR) of zero lag. If $\boldsymbol{x} \in \mathbb{R}^N$ is the multivariate vector of observations at a given time $t$,

$$\boldsymbol{x}(t+1) = \boldsymbol{F}\boldsymbol{x}(t) + \boldsymbol{e}(\boldsymbol{t+1}) \tag{1}$$

with $\boldsymbol{F} \in \mathbb{R}^{N \times N}$ a matrix of the connection between variables and $\boldsymbol{e}$ additive Gaussian noise between variables with zero mean and identity covariance.

We consider the ongoing brain activity in resting-state as a stationary process. If $\boldsymbol{X} \in \mathbb{R}^{N \times t}$ is the matrix of the observed time series and $\boldsymbol{E} \in \mathbb{R}^{N \times t}$ then

$$\boldsymbol{X} = \boldsymbol{F}\boldsymbol{X} + \boldsymbol{E} \Leftrightarrow \boldsymbol{X} = (\boldsymbol{I} - \boldsymbol{F})^{-1}\boldsymbol{E} \tag{2}$$

where $\boldsymbol{I}$ is the $N \times N$ identity matrix. Thus, the covariance of the observed time series, $\boldsymbol{\Sigma}$, is given by:

$$\boldsymbol{\Sigma} = \frac{1}{r}\boldsymbol{X}\boldsymbol{X}^T = (\boldsymbol{I} - \boldsymbol{F})^{-1}\mathrm{cov}\boldsymbol{E}(\boldsymbol{I} - \boldsymbol{F})^T = ((\boldsymbol{I} - \boldsymbol{F})^T(\boldsymbol{I} - \boldsymbol{F}))^{-1} \tag{3}$$

Note that $\mathrm{cov}\boldsymbol{E} = \boldsymbol{I}$ and $\boldsymbol{B} = \boldsymbol{I} - \boldsymbol{F}$ is a matrix square root of the inverse covariance, which we call the interaction matrix.

$$\boldsymbol{\Sigma^{-1}} = \boldsymbol{B}^T\boldsymbol{B}. \tag{4}$$

The problem to solve is known as covariance selection problem, which is the problem of computing the maximum likelihood estimate of the inverse covariance matrix of a multivariate Gaussian variable, subject to conditional independence constrains.

### 2.2 Markov structure.

Conditional independence between variables is given by the zeros in the precision matrix. Estimating from the fMRI data a sparse precision matrix reduces the small-sample estimation error present in the empirical covariance matrix [12]. In fact, the number of functional connectivity parameters is much greater than the number of samples: $t < \frac{1}{2}N\,(N+1)$. This results in a large estimation error of the sample covariance matrix [13, 12]. We use anatomical connections that fail to be significantly positive across subjects to impose the Markov structure of the fMRI model [1]. The maximal likelihood estimate of $\boldsymbol{K}$ is then computed using the iterative proportional scaling algorithm [13].

### 2.3 Imposing definite positive predictions.

To parameterize a valid Gaussian model, the predicted precision matrix must be positive definite. This condition on the output space corresponds to constraints on the coefficients of $\boldsymbol{K}$. However, we cannot predict independently these coefficients and ensure that the resulting matrix will be in $\mathcal{S}ym_N^+$. Thus, rather than predicting $\boldsymbol{K}$, we predict a square root, the interaction matrix, $\boldsymbol{B}$, that is not

constrained. Here, we use the Cholesky decomposition of the precision matrix $\boldsymbol{K}$ to estimate $\boldsymbol{B}$. The Cholesky decomposition is not invariant to a permutation of the rows and columns of the input matrix $\boldsymbol{K}$. We use the approximate minimum degree (AMD) ordering [14], which provides a permutation of $\boldsymbol{K}$ favoring a sparser Cholesky decomposition. This permutation depends only on the support of the matrix $\boldsymbol{K}$, and thus it is identical across subjects. Note that we are interested in predicting correlation and not covariance, thus, we rescale the diagonal of $\boldsymbol{B}$ to ones: $\tilde{\boldsymbol{B}} = \boldsymbol{B}\, diag(\boldsymbol{B})^{-1}$. This amounts to setting the innovation terms of the MAR to one.

### 2.4 Statistical learning.

We use a multivariate linear model between all the anatomical connections $\boldsymbol{a} = \{\boldsymbol{A}_{i,j}\}$ and the coefficients of the matrix $\tilde{\boldsymbol{B}}$, $\boldsymbol{b} = \{\tilde{\boldsymbol{B}}_{i,j}\}$. The learning problem takes the form of multiple regressions: for the $k^{\text{th}}$ functional connection, $b_k$,

$$b_k = \beta_{k,0} + \sum_{m=1}^{M} \beta_{k,m}\, a_m, \tag{5}$$

where $M$ is the number of non zero connections, $\beta_0$ is the intercept, and $\beta_k$ are the coefficients relating the functional connection $\boldsymbol{b}_k$ to the whole-brain anatomical connectivity, $\boldsymbol{a}$. There are many more candidate anatomical connections than subjects: we are in high-dimensional setting. Therefore we resort to Lasso, which is sparse $\ell_1$ penalized regression.

$$\hat{\boldsymbol{\beta}}_k = \underset{\boldsymbol{\beta}}{\operatorname{argmin}} \left( \sum_{s=1}^{S} \left( b_k^s - \sum_{m}^{M} \beta_m\, a_m^s \right)^2 + \lambda \sum_{m=1}^{M} |\beta_m| \right) \tag{6}$$

To simplify the formulation, we omit the intercept $\beta_0$. Lasso performs both variable selection and prediction [15]. Over classical least square regression it offers two major advantages that are very useful in modeling brain connectivity: Firstly, it improves prediction by setting some coefficients to zero. This results in removing noisy and irrelevant variables and thus reducing the total variance. Secondly, it allows the selection of the most relevant variables and thus it links each functional connection with a subset of structural connection in a data driven way. The correct predictors are identified with high probability even when the number of variables is higher than the number of observation under the assumption that the true model is sparse [16]. We use the LARS algorithm, implemented in the scikit-learn toolbox [17].

## 3 Model selection and identification

In this section, model selection guarantees that the optimum Markov support is selected based on cross-validation and an intrinsic metric suitable to quantify distance between symmetric positive definite matrices $\mathcal{S}ym_N^+$. Finally, model

identification based on randomised Lasso extract the most robust associations between function and structure and provides a sound method to quantify confidence for these measurements.

### 3.1 Model selection metric.

We work on the space of sparse Gaussian models, parametrized by correlation or precision matrices, symmetric definite positive matrices. This space, $\mathcal{S}ym_N^+$, is not a vector space. The standard Euclidean distance on matrices, the Frobenius norm, does not account for the geometry of this space. Thus, it is ill suited to quantify prediction errors. However, $\mathcal{S}ym_N^+$ can be parametrized as a Riemannian manifold using an intrinsic metric [1, 18]:

$$d_{AI}(\boldsymbol{C}, \boldsymbol{D})^2 = \operatorname{tr}\big(\log \boldsymbol{C}^{-\frac{1}{2}} \boldsymbol{D}\, \boldsymbol{C}^{-\frac{1}{2}}\big)^2 \tag{7}$$

This metric is invariant under affine scaling and inversion of the matrices, and is thus independent of the parameterization of the Gaussian models. In other words, it gives the same prediction error on the correlation matrices and on the precision matrices.

### 3.2 Randomized Lasso.

We use the randomized Lasso [19] to identify non-zero coefficients $\beta_k$. It is a generalization of Lasso with better recovery properties. The randomized Lasso estimate is computed by solving the Lasso problem with weights $W_j$ random within specified bounds:

$$\hat{\boldsymbol{\beta}}_k = \underset{\boldsymbol{\beta}}{\operatorname{argmin}} \left( \sum_{s=1}^{S} \big(b_k^s - \sum_{m}^{M} \beta_m\, a_m^s\big)^2 + \lambda \sum_{m=1}^{M} \frac{|\beta_m|}{W_m} \right) \tag{8}$$

This randomized penalization regression is solved many times. The probability that a functional connection is related to a anatomical connection is then given by the fraction of times the coefficient is selected during the repetitions.

Randomised Lasso introduces proper regularisation so that a certain family-wise type I error rate (false discoveries) in multiple testing can be conservatively controlled for finite sample size. We do not simply select a set of connections that corresponds to the initial set of regularisation parameters, $\lambda$. Instead $\lambda$ perturbed many times and the connections that occur in a large fraction of the results are selected. Therefore, the initial set of regularisation parameters, $\lambda$, have not a very strong influence on the results.

Randomised Lasso has been also proven to be variable selection consistent even if the conditions needed for consistency of the original Lasso method are violated [19]. Consistency refers to how well the sparse model retrieved by Lasso relates to the true model. The condition that it is necessary and sufficient to guarantees Lasso consistency can be easily violated in practical problems. For example, if an irrelevant predictor is highly correlated with the predictors in

| Markov model sparsity | | 80% | 70% | 60% | 50% | 40% | 30% | 20% | 10% |
|---|---|---|---|---|---|---|---|---|---|
| Random order | $d_{AI}$ | 25.0 | 26.0 | 27.8 | 29.5 | 34.1 | 39.2 | 50.6 | 67.2 |
| | std | 32.4 | 8.0 | 8.2 | 8.4 | 8.2 | 8.1 | 8.1 | 8.0 |
| AMD order | $d_{AI}$ | 31.3 | 24.5 | 24.0 | 25.3 | 26.1 | 27.3 | 42.5 | 63.2 |
| | std | 49.3 | 8.2 | 8.4 | 8.4 | 9.0 | 9.5 | 9.6 | 9.8 |

Table 1: Prediction performance, measured with the $d_{AI}$ metric, for different sparsity of the Markov structure and under different ordering of $\boldsymbol{K}$.

the true model, Lasso cannot distinguish it from the true predictors given any amount of data and any regularisation [19]. Randomised Lasso needs a much weaker assumption to be consistent. It requires that the full model in Eq. 5 can be approximated by a much lower-dimensional submodel of coefficients so that model selection makes sense [20].

## 4 Experimental results

Brain connectivity analysis was performed in 26 normal adults. rs-fMRI: T2*-weighted gradient EPI sequence, TR/TE=2000/30, 31 ascending slices with thickness $3.25mm$, gap $0.75mm$, voxel size 2.5x2.5x4$mm$, flip angle 90, FOV 280x220x123$mm$, matrix 112x87. DWI: 64 non-collinear directions, in 72 slices, slice thickness $2mm$, FOV $224mm$, matrix 128x128, voxel size 1.75x1.75x2$mm^3$, b-value 1000 $s/mm^2$. High resolution T1-weighted whole-brain structural images were also obtained in all subjects.

FSL was used for image pre-processing of both diffusion weighted (DWI) and fMRI images [21]. BOLD fluctuations are profound in gray matter, while DTI is more reliable in delineating white matter fibers. Hence, we are interested in defining cortical ROIs that are located in gray matter and they are defined according to widely used anatomical atlas [22]. Cortical parcellation is obtained with the fusion of atlas-based [22] and tissue based segmentation [23].

To construct corresponding functional networks the fMRI signal was averaged across voxels within each area. The signal in CSF and white matter has been also averaged and the six motion correction parameters were estimated with FEAT, FSL [21]. All these eight parameters were accounted in the estimation of the covariance matrix. Tracts between regions are identified using a standard probabilistic algorithm available as part of FSL [21, 24]. We estimate the local diffusion anisotropy by determining the diffusive transfer between voxels using the orientation distribution function (ODF) [25].

To set the level of support that gives the optimum prediction performance, we vary the threshold on the t-test so that the percentage of connections selected ranges from 10% to 80%. We also compare two choices of ordering for the Cholesky decomposition of the precision matrix $K$: random ordering and model averaging, or AMD ordering for sparser Cholesky factors. Cross-validation results (Table 1) show that the optimum sparsity for the Markov structure corresponds to selecting 60% of the connections, and that AMD ordering is to be preferred to averaging on random orderings.

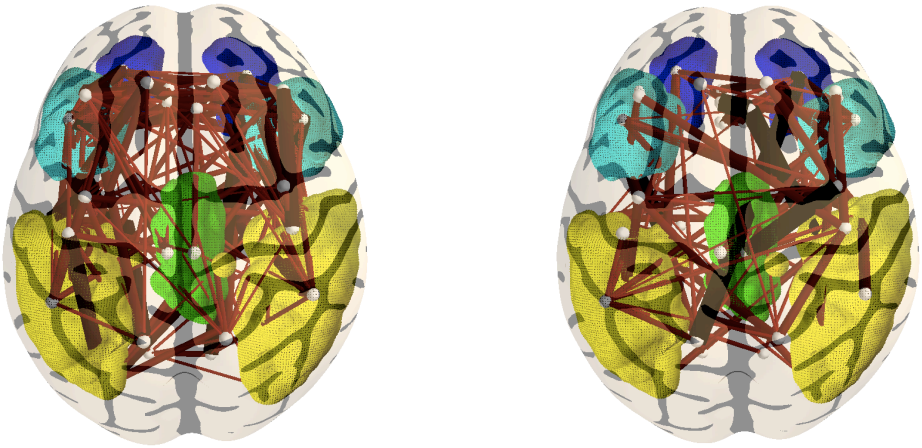

Fig. 1: Structural connections associated with the default mode network: **left** random order; **right** AMD.

Once a percentage of 60% structural connections included has been identified as the optimum Markov structure, we run model identification across all the 26 subjects with this support. Fig. 1 shows structural connections associated with the default mode network. With yellow is represented the lateral parietal cortex, green areas represent the posterior cingulate gyrus (PCC), blue and light blue represent the medial prefrontal and orbito-frontal areas, respectively. The diameter of the tubes is associated with the probability of the connection to be selected.

## 5 Conclusions

We use the probabilistic framework introduced in [1] to learn a predictive model from anatomical to functional brain connectivity. Here, we use cross-validation to set the properties of the Markov model of fMRI: filling factor, and ordering of the nodes in the MAR. As we are interested in recovering the relevant anatomo-functional links, we also introduce randomized Lasso that can identify better non-zero coefficients in linear models with correlated designs. Randomised Lasso assign a probability for each structural selected connection that depicts the probability each connection to be selected. With sensible choices, in a range of the cutoff, results vary very little. This is a significant step towards interpreting the results compared with the original Lasso. Original Lasso has a coefficient assigned to each selected connection which can be either positive or negative and it is difficult to intuitively interpret their significance.

## References

1. F. Deligianni, et al. : A probabilistic framework to infer brain functional connectivity from anatomical connections. IPMI (2011) 296–307

2. O. Sporns: The non-random brain: efficiency, economy, and complex dynamics. Front Comput Neurosc **5** (2011) 5
3. J. Burns: An evolutionary theory of schizophrenia: Cortical connectivity, metarepresentation, and the social brain. Behavioral and Brain Sciences **27**(6) (2004) 831
4. R. Muller: The study of autism as a distributed disorder. Mental retardation and developmental Disability Research **13**(1) (2007) 85–95
5. L. Pollonini, et al. : Information communication networks in severe traumatic brain injury. Brain Topogr **23**(2) (2010) 221–226
6. E. Bullmore and O. Sporns: Complex brain networks: graph theoretical analysis of structural and functional systems. Nat Rev Neurosci **10** (2009) 186–198
7. D. Zhang and M. E. Raichle: Disease and the brain's dark energy. Nat Rev Neurol **6**(1) (2010) 15–28
8. C. Honey, et al. : Predicting human resting-state functional connectivity from structural connectivity. P Natl Acad Sci Usa **106**(6) (2009) 2035–2040
9. P. Hagmann, et al. : Mapping the structural core of human cerebral cortex. PLoS Biol **6**(7) (2008) 1479–1493
10. M. D. Greicius, et al. : Resting-state functional connectivity reflects structural connectivity in the default mode network. Cerebral Cortex **19**(1) (2009) 72–78
11. M. van den Heuvel, et al. : Microstructural organization of the cingulum tract and the level of default mode functional connectivity. J Neurosci **28**(43) (2008) 10844–10851
12. G. Varoquaux, et al. : Brain covariance selection: better individual functional connectivity models using population prior. NIPS (2010)
13. S. Lauritzen: Graphical models. Oxford University Press, USA (1996)
14. P. Amestoy, et al. : An approximate minimum degree ordering algorithm. SIAM Journal on Matrix Analysis and Applications **17**(4) (1996) 886–905
15. R. Tibshirani: Regression shrinkage and selection via the lasso. J Royal Statist Soc B **58**(1) (1996) 267–288
16. D. Donoho: For most large underdetermined systems of linear equations the minimal l1-norm solution is also the sparsest solution. Comm. Pure Appl. Math. **59**(6) (2006) 797–829
17. F. Pedregosa, et al. : Scikit-learn: Machine learning in Python. The Journal of Machine Learning Research **to appear** (2011) pub ahead of print
18. G. Varoquaux, et al. : Detection of brain functional-connectivity difference in post-stroke patients using group-level covariance modeling. In: MICCAI. (2010)
19. N. Meinshausen and P. Buhlmann: Stability selection. Journal of the Royal Statistical Society: Series B **27** (2010) 417–473
20. C.-H. Zhang and J. Huang: The sparsity and bias of the lasso selection in high-dimensional linear regression. Annals of statistics **36** (2008) 1567–1594
21. S. Smith, et al. : Advances in functional and structural MR image analysis and implementation as fsl. NeuroImage **23** (2004) 208–219
22. P. Aljabar, et al. : Multi-atlas based segmentation of brain images: atlas selection and its effect on accuracy. NeuroImage **46**(3) (2009) 726–38
23. K. Friston: Statistical parametric mapping: the analysis of functional brain images. Academic Press (2007)
24. T. Behrens, et al. : Characterization and propagation of uncertainty in diffusion-weighted MR imaging. Magnet Reson Med **50**(5) (2003) 1077–1088
25. E. Robinson, et al. : Identifying population differences in whole-brain structural networks: a machine learning approach. NeuroImage **50**(3) (2010) 910–919